ELSEVIER

Cement & Concrete Composites 25 (2003) 491–502

Cement & Concrete Composites

www.elsevier.com/locate/cemconcomp

Chloride-induced corrosion on reinforcing steel: from the fundamentals to the monitoring techniques

M.F. Montemor *, A.M.P. Simões, M.G.S. Ferreira

Grupo de Corrosão e Efeitos Ambientais, DEQ, Instituto Superior Técnico, Av. Rovisco Pais, 1049-001 Lisboa, Portugal

Abstract

One of the most important causes for reinforcing steel corrosion is the presence of chloride ions. They cause localised breakdown of the passive film that initially forms on steel as a result of the alkaline nature of the pore solution in concrete. The harmful chloride ions can be originated from the use of contaminated mix constituents or from the surrounding environment. The determination of a critical level, above which serious problems can occur, has been one of the main goals of investigation. Unfortunately, it is difficult to establish such a value since the chloride level is influenced by several factors. Thus, after concrete contamination, it is of fundamental importance to follow the activity of chlorides and the state of the reinforcing rebars. In this respect, the use of electrochemical techniques such as polarisation resistance, electrochemical impedance, galvanostatic pulse and potential measurements have shown to be powerful tools. Nevertheless, the interpretation of the results becomes sometimes a difficult task. A large number of authors have dedicated several studies to the interpretation of such measurements and a highly dispersed number of interpretations can be found in literature. The aim of this paper is to present an overview on the state-of-the-art of the most important aspects of the corrosion process initiated by chlorides, its development and monitoring techniques.

Keywords: Concrete; Reinforcement corrosion; Chlorides; Corrosion monitoring

1. Introduction

The use of cement, the most important ingredient of concrete, is known since the construction of pyramids in old Egypt, where it was used as a binding agent. Nowadays concrete is one of the most widely produced materials on the earth, with consumption above dozens of billions of tons. The concrete industry involves millions of euros being the basis of the modern society development. Contrary, to the common belief, concrete is not free of severe degradation problems. Apart from structural design failures, the most important cause of concrete degradation is the corrosion of the reinforcing steel. This problem has reached alarming proportions in the past three decades, leading to very high repair costs, sometimes above the initial construction cost, or in extreme situations, to the final collapse of the structure.

The most important causes of reinforcement corrosion are (i) localised depassivation of the reinforcing steel due to the ingress of chloride ions and (ii) complete depassivation of the reinforcement due to acidification of the interstitial solution in consequence of reactions of the cement matrix with carbon dioxide present in the atmosphere.

The harmful chloride ions may be present in concrete, as result of the use of contaminated ingredients on the manufacture of the mix, or as result of an external contamination prior to construction. This situation arises from exposure of the structures to water and marine atmospheres or to the use of de-icing salts (NaCl, $CaCl_2$ and $MgCl_2$) a necessary practice in cold climates.

After initiation of the corrosion process, the accumulation of corrosion products (iron oxides and hydroxides), occupying a volume several times larger than that of the original iron [1] leads to internal stresses that result in cracking and spalling of the concrete cover. At this stage the intrusion of aggressive agents, oxygen and

* Corresponding author. Tel.: +351-21-8417234.
E-mail address: pacfatima@alfa.ist.utl.pt (M.F. Montemor).

0958-9465/03/$ - see front matter
doi:10.1016/S0958-9465(02)00089-6

humidity is facilitated and the next step can be the total loss of the structural integrity.

2. Chloride-induced corrosion of reinforcement

2.1. The corrosion process

Corrosion is an electrochemical process with cathodic and anodic half-cell reactions. In the absence of chlorides and in good quality concrete, in which the pH is usually in the range 12.5–13.5, the anodic reaction (1) leads to the formation of iron cations, according to:

$$Fe \rightarrow Fe^{2+} + 2e^{-} \quad (1)$$

This reaction is balanced by the cathodic reduction of oxygen, which produces hydroxyl anions according to reaction (2).

$$1/2O_2 + H_2O + 2e^{-} \rightarrow 2OH^{-} \quad (2)$$

The products of both reactions combine together and in a last stage they produce a stable film that passivates the reinforcing steel. The stability of this film depends essentially on the oxygen availability that controls reaction (2) and on the pH of the interstitial solution in the interface steel/concrete [2].

The nature of the passive film formed on iron in alkaline media, such as the one in concrete, is attributed to the presence of Fe_3O_4 and/or Fe_2O_3 [3–5] or to the presence of γ-FeOOH [6–9]. Some of these compounds were identified by X-ray diffraction analysis performed on steel bars [10].

The passive film was also studied by other researchers [11–13], who suggested that protection is provided by the presence of a $Ca(OH)_2$-rich layer that adheres to the steel, hindering the cathodic reaction.

Another explanation for the passivation of reinforcing steel assumes that the passive film is composed of different regions: one outer $Ca(OH)_2$ rich layer, on the concrete side, which provides only limited protection and an inner Fe oxide/hydroxide layer that passivates the steel [14]. Montemor et al. [15] have studied the composition of the passive film by means of Auger and X-ray photoelectron spectroscopy (XPS) and found the presence of a calcium rich layer in the outermost part of the film as shown in Fig. 1. They also observed the presence of FeOOH, whose concentration decreased with depth. At the same time the other forms of iron (Fe_2O_3, Fe^{2+} and Fe^0) tend to increase as the analysis approaches the steel substrate. The authors also reported that the presence of chlorides results in thicker films, where the contents of FeOOH and H_2O tend to increase. Fig. 2 depicts the oxygen spectra obtained by XPS on steel samples immersed during one week in cement paste solutions with different chloride contents.

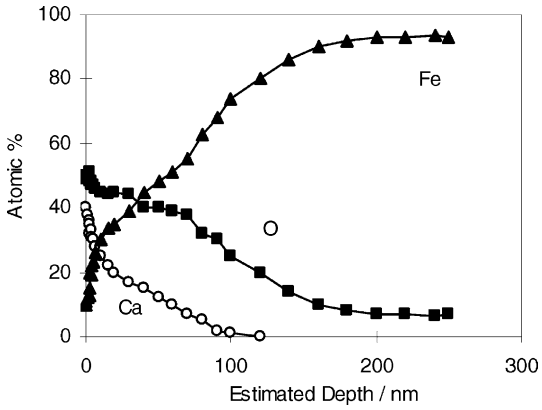

Fig. 1. Auger depth profile obtained on steel immersed in cement paste solution for one week.

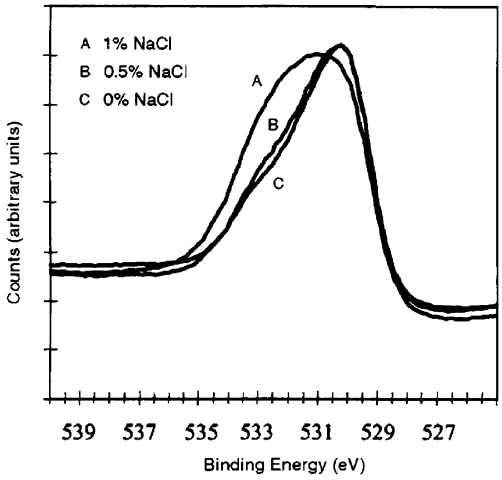

Fig. 2. O 1s XPS spectra obtained on steel immersed for one week in cement paste solutions with various contents of NaCl [15].

The shape of the peak reveals a high energy broadening with chloride concentration, as a consequence of the formation of more hydrated iron compounds.

In the presence of chlorides, the passive film is locally destroyed and a process of localised corrosion is then initiated. The mechanism of breakdown was studied by a large number of authors. Jovancicevic et al. [16] described and criticised a number of models proposed to explain the breakdown of the passive film by the chloride ions. The authors reported three general models: (i) adsorption-displacement, (ii) chemico-mechanical and (iii) migration-penetration.

The first model was initially proposed by Leckie and Uhlig [17,18] and Kolotorkyn [19] and suggests that breakdown involves adsorption of Cl^- with simultaneous displacement of O^{2-} from the passive layer, leading to initiation of film destruction.

In the second model, Hoar [20] proposed that chloride ions lower the interfacial surface tension, which

results in the formation of cracks and flaws, when the repulsive forces between adsorbed ions are sufficiently large. This situation weakens the passive film. This view was further developed by Sato [21], who provided a more detailed picture of the model.

Generally, the third model involves ion migration through an exchange process via cation vacancies and O^{2-} or OH^-. Chao et al. [22] developed this model and suggest that Cl^- reaches the steel occupying O^{2-} vacancies, leading to the formation of complexes with Fe^{2+}. The decrease of oxygen vacancies at the film/solution interface caused by Cl^- leads to the formation of voids due to faster iron dissolution, leading to pit growth. Pou et al. [23] suggested that absorbed Cl^- ions displace water molecules (or OH^-), which according to Grady and Bockris [24] are the basis of the passive film. This results in the formation of soluble iron complexes and conversion of the amorphous layer into a crystalline layer. The solubility of these products release chlorides, making them available for further reaction with iron. The process results in localised acidification and finally in the breakdown of the passive film. The formation of iron oxides and hydroxides in these sites, occupying larger volume than the original iron leads to the generation of internal forces that decrease the adhesion at the steel/concrete interface.

2.2. The chloride threshold content

Following the discussion on the passive film breakdown it is clear that the harmful chlorides must reach the steel in the form of Cl^-. Concrete, however, has the capacity to bind the chloride ions leading to the formation of calcium chloroaluminate (Friedel's salt), a complex between the hydration products of cement and chloride: $[Ca_2Al(OH)_6]Cl \cdot 2H_2O$ or $C_3ACaCl_2 \cdot 10H_2O$, where C_3A denotes tricalcium aluminate. These salts partly immobilise chlorides and consequently determine the chloride level required to initiate the corrosion process.

Suryavanshi et al. [25] have studied the mechanism of Friedel's salt formation and have proposed two approaches: one based on an adsorption mechanism and the other based on an anion-exchange mechanism. In the first one, Friedel's salt is formed due to the adsorption of the bulk Cl^- present in the pore solution into the interlayers of the principal layer $[Ca_2Al(OH^-)_6 \cdot 2H_2O]^+$ of the aluminoferrite structure to balance the charge. Associated with this process, a cation (usually that associated with Cl^-) is also removed from solution to maintain ionic charge neutrality and binds with the calcium–silicate–hydrate (C–S–H) lattice. In the second one, Cl^- is bound by releasing an equivalent amount of OH^- from the aluminoferrite hydrates into the pore solution, thereby increasing interstitial solution pH. The chlorides then replace hydroxyl in the interlayers of the aluminoferrite hydrates. They also found that bound chlorides are dependent on the chloride salt cation.

The microstructure of chloroaluminates plays an important role in the process of chloride fixation [26]. If the chloride concentration rises above the binding capacity of concrete, it is no more fixed and becomes available to initiate the corrosion process. This simple model originated the concept of chloride threshold level, which is defined as the chloride concentration at the steel/concrete interface that results in a significant corrosion rate, leading to corrosion-induced deterioration [27].

The establishment of the chloride threshold level has been one point of increasing interest. However, this parameter is affected by a large number of factors characteristic of the steel/concrete system, such as:

- the interstitial solution chemistry and pH;
- water to cement ratio;
- concrete composition, namely, cement type use of additives, such as fly ash and other mineral admixtures;
- pore and capillary structure;
- curing period and curing and exposure temperature.

Glass et al. [28,29] published an interesting discussion on the chloride threshold level. These works report several values obtained by a number of authors in different conditions: (i) outdoors concrete structures and (ii) laboratory experiments using mortar, concrete, pastes and solutions. From those values it was shown that the total chloride content, expressed in wt.% cement, are in the range of 0.17–2.5, thus changing by about 15 times. These strong differences clearly illustrate the difficult in establishing such parameter. Moreover, according to the recent works of Glass et al. [30,31] the chlorides bound in concrete also play an important role in the corrosion process, since they affect the rate of chloride ingress and the chloride threshold value and thus, the time to corrosion initiation. According to the authors [30], chloride binding by cement generates higher concentration gradients for longer periods in the surface zone, thereby increasing the average velocity and quantity of chlorides entering the concrete through diffusion as shown in Fig. 3. The increase on the chloride binding capacity only results in a decrease of the total chloride content at depths larger than 50 mm or times longer than 50 years. The net effect is an increase in the total chloride content (bound plus free) near surface and a reduction in total chloride content with depth. The authors [30,31] concluded that the bound chlorides are able to participate in the corrosion initiation, because a fall in pH may induce dissolution of the complexing phases, releasing free chloride ions.

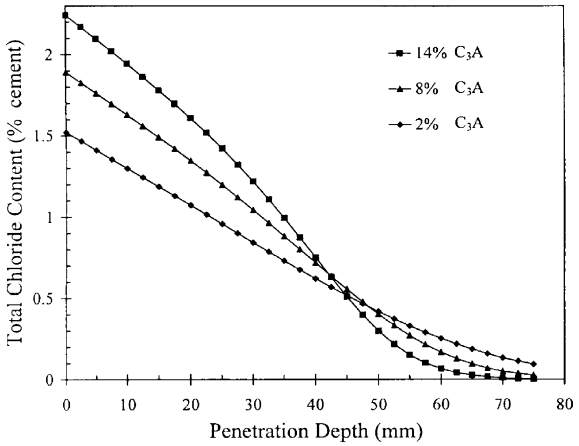

Fig. 3. Predicted total chloride profiles after 50 years corresponding to cements with varying C3A contents [30].

From the discussion above, it is clear that quantification and prediction of the chloride content in concrete can be a difficult task. The process is affected by a large number of variables and the error involved can be significantly high. Thus, the need of constant monitoring of the state of the reinforcing steel in order to detect corrosion onset becomes of fundamental importance.

3. Monitoring techniques

3.1. Potential measurements

The detection of corrosion by using potential measurements is one of the most typical procedures for the routine inspection of reinforced concrete structures. The technique is very well known, being described in the American National Standards ANSI/ASTM C876. An oversimplified interpretation of the potential readings is described by:

E_{corr} (vs. Cu/$CuSO_4$)	Probability of corrosion
<-0.35 V	>95%
>-0.20 V	<5%
-0.20 to -0.35 V	≈50%

Potential readings, however, can be more negative than −350 mV (SCE), without significant presence of corrosion. This effect is closely associated with polarisation phenomena induced by limited oxygen diffusion as stated by some authors, such as Arup [32] and Elsener and Böhni [33]. Due to restricted oxygen access the steel becomes active, but the corrosion process does not proceed and the measured potential can fall to values that may attain −1 V vs saturated calomel electrode (SCE) [32]. Fig. 4 illustrates a situation where permanent immersion of the concrete samples leads to open circuit potential readings lower than −600 mV (SCE). After air exposure and consequently free oxygen access the potential increased to values around −400 mV (SCE), typical of corrosion activity as stated by other monitoring techniques [34].

Another factor affecting the potential readings is the presence of high resistive layers of concrete [35]. In this situation, if the potentials are taken remote from the reinforcement, due to concrete cover, they are in fact "mixed potentials". This means that the cathodic areas affect potential readings and, therefore, they are less negative than the potential adjacent to the steel. The magnitude of this effect can lead, in theory, to differences of up to 200–300 mV [35]. Alonso et al. [36] have reported that the potential values are dependent on the conductivity of the formed corrosion products and on the age of concrete.

Stray currents [37] and generation of junction potentials [35,37] can also affect the potential readings.

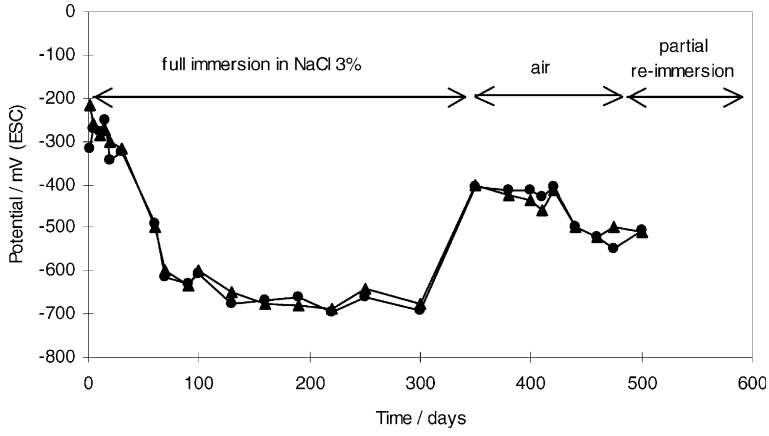

Fig. 4. OCP evolution on steel embedded in concrete samples exposed to different environments: full immersion, air drying and partial re-immersion [34].

Other factors affecting potential measurements include reference electrode position, cement type and the presence of cracks [38]. Nevertheless, the technique is widely used and works as a first approach to corrosion detection. However, quantification and reliable prediction of the corrosion rate needs the use of other electrochemical techniques.

3.2. Polarisation resistance measurements

Measurement of DC polarisation resistance with ohmic drop compensation has been applied since 1970s and gives information on the corrosion rate. The fundamentals of the technique are well known and are based on the Stern–Geary equation [39]:

$$I_{corr} = B/R_p, \text{ where } B = \beta_a\beta_c/[2.3(\beta_a + \beta_c)] \quad (3)$$

with: R_p denoting the polarisation resistance and β_a and β_c the anodic and cathodic Tafel constants, respectively.

In concrete, however, the main difficulty in the use of the technique arises from irregular distribution of the electrical signal applied via the counter electrode of much smaller dimensions than the reinforced concrete structure under test. Instead of a uniform distribution over the whole metallic system, the electrical signal tends to vanish with increasing distance from the counter electrode location. To solve this problem Feliu et al. [40,41] and Gonzalez et al. [42] developed an approach based on a "transmission line" model. The authors propose an analytical solution for estimating the polarisation resistance and check their validity by comparing the analytical solutions with direct measurements of polarisation resistance (R_p) obtained under conditions projected to achieve an uniform distribution of the signal applied to the reinforcement. The model demonstrates that the response of a large reinforced concrete structure to an electrical signal applied via a counter electrode of much smaller dimensions can be modelled based on the response of a transmission line. Two approaches were derived from the model. The first one uses the response in current resulting from the application of a potential step to the reinforcement with the aid of a smaller counter electrode, placed on the concrete beam. The second one is based on the decrease of the potential applied in this manner in terms of distance from the referred counter electrode.

The model clearly differentiates between the behaviour of the steel in the passive state ($R_p \approx 10^5$–$10^6\ \Omega\,cm^2$ e.g. concrete without chlorides) and in an active state ($R_p \approx 10^3$–$10^4\ \Omega\,cm^2$ e.g. concrete with 3% $CaCl_2$). This model was adopted by a number of authors as a way to estimate the corrosion rate [43].

The aforementioned problems of lack of uniformity and of knowledge of the area over which the electrical signal distributes become minimal if the signal could be confined to a given area of the structure located below the counter electrode. This can be achieved by the means of the guard ring technique. This consists of a second counter electrode located concentrically around the first one, which allows the confinement of the signal in a well-defined region of the structure.

Fig. 5 depicts the schematic representation of the guard ring technique [44]. Both counter electrodes are maintained at the same electrical potential with respect to the working electrode (steel), which allows measurement of current flowing from the central counter electrode. Therefore, while a central auxiliary electrode locally polarises the bars, another one—concentrical to former—provides polarisation to the rest of the rebar around the area affected by the central one. Since the central electrode's current is known, as well as the area of reinforcement affected by it, determination of R_p is made immediately.

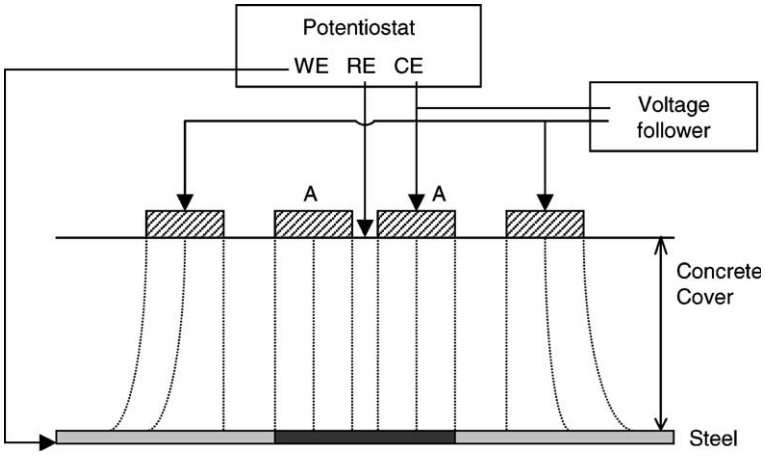

Fig. 5. Schematic representation of the use of the guard ring. It shows an ideal case, in which the current flowing from the central counter electrode (A) is directed exclusively to polarising the portion of the rebar beneath it (Discontinues lines represent current lines.) [44].

Feliu et al. [44] demonstrated that the technique could be successfully applied to active reinforced structures; however, in passive structures some underestimation of the R_p values may occur.

The accuracy and reproducibility of R_p measurements by means of guard ring electrodes was also investigated by Sehgal et al. [45]. They tested the effect of a number of variables, such as effect of wetting, surface morphology and presence of resistive layers. The study reveals that accuracy can be improved by using a planar concrete surface, decreasing the contact resistance between probe and concrete surface, using water or other conductive non-aggressive path, making measurements after steady-state potential was reached and symmetric positioning of the probe over the rebars.

The guard ring technique is nowadays well established and a number of commercial devices are available. Among these some are referred in literature: GECOR, which works on the principle of linear polarisation and uses an external ring for current confinement, polarising the rebar by 10–30 mV [46] and CAPCIS that uses the same principle for current confinement and possesses a dry contact system composed of a conductive carbon layer [47]. Some of these devices were tested in situ [48]. It was confirmed that the guard ring technique provides signal confinement in situ, but a few limitations, such as dependence on concrete resistivity were observed. In certain situations underestimating of the corrosion rates was detected [49].

3.3. Electrochemical impedance

Electrochemical impedance spectroscopy (EIS) is a technique working in the frequency domain. The basic concept involved in EIS is that an electrochemical interface can be viewed as a combination of passive electrical circuit elements, i.e., resistance, capacitance and inductance. When an alternating voltage is applied to these elements, the resultant current is obtained by using the Ohm's law. In a simple way, impedance can be thought of as the resistance of a circuit to an alternating waveform. From these basic concepts to nowadays, the technique has found increasing applications, becoming a tool of fundamental importance in corrosion research. EIS provides information on the mechanism of the corrosion reactions, surface films, adsorbed intermediates etc. It can be used in low conductivity media, such as concrete, without system perturbation.

The first attempts at the use of EIS for monitoring corrosion in reinforced concrete were made by John et al. [50]. The authors proposed the circuit depicted in Fig. 6(a) and applied EIS to concrete samples immersed in seawater. The impedance response in the low frequency range was correlated with the charge transfer process, whereas the response at high frequencies was assigned to the presence of a surface film.

Later, Gonzalez et al. [51] compared EIS response with linear polarisation and observed that EIS allows determination of some characteristics of the corrosion process. They noted that accuracy in the determination of R_p was similar or even smaller (if extrapolations are needed) than other techniques, namely linear polarisation resistance.

Another approach for the interpretation of the steel/concrete system was published by Macdonald et al. [52]. The author described the system response based on a transmission line model as shown in Fig. 6(b). This model assumes that the electrical properties of steel and concrete are purely resistive, with concrete resistivity (but not that of steel), being dependent on the position due to matrix inhomogeneity. On the other hand, the model assumes that the interface is reactive due to the existence of capacitive, pseudo-capacitive and diffusional components. The model shows that the real and imaginary part of the impedance response and the phase angle at low frequencies allow detection and localisation of corrosion. An identical model was adopted by Saguës [53].

Wenger and Galland [54] proposed the circuit depicted in Fig. 6(c), in which the response at high frequencies is associated with the presence of a lime-rich film formed on the steel surface. This model correlates well with the impedance response of small specimens. However, for larger structures, the model is no longer valid and the authors adopted another one based on a transmission line model.

Dhouibi et al. [55] proposed another approach shown in Fig. 6(d), which includes the following items: (i) products formed directly on steel surface, (ii) products resulting from reaction between corrosion products and cement paste and (iii) the bulk concrete cover. The model shows a good agreement between experimental data and calculated Nyquist diagrams.

When concrete becomes active due to corrosion initiated by the chloride ion, usually there is formation of active areas in electrical contact with passive areas, leading to the formation of macrocells. This situation led to some developments in the equivalent circuits in order to simulate the process. Nöggerath and Böhni [56] proposed a circuit to describe the development of macroelements in reinforcing steel. Their study shows that small corrosion spots surrounded by large passive areas cause such high resistances that the impedance spectra become controlled by the passive part. On the other hand, in the presence of large active areas the determination of R_p is difficult due to the presence of diffusion phenomena. This situation makes it necessary to introduce a model where there is a continuous change in the ratio of the passive/active areas. Keddam et al. [57] also studied the effect of the

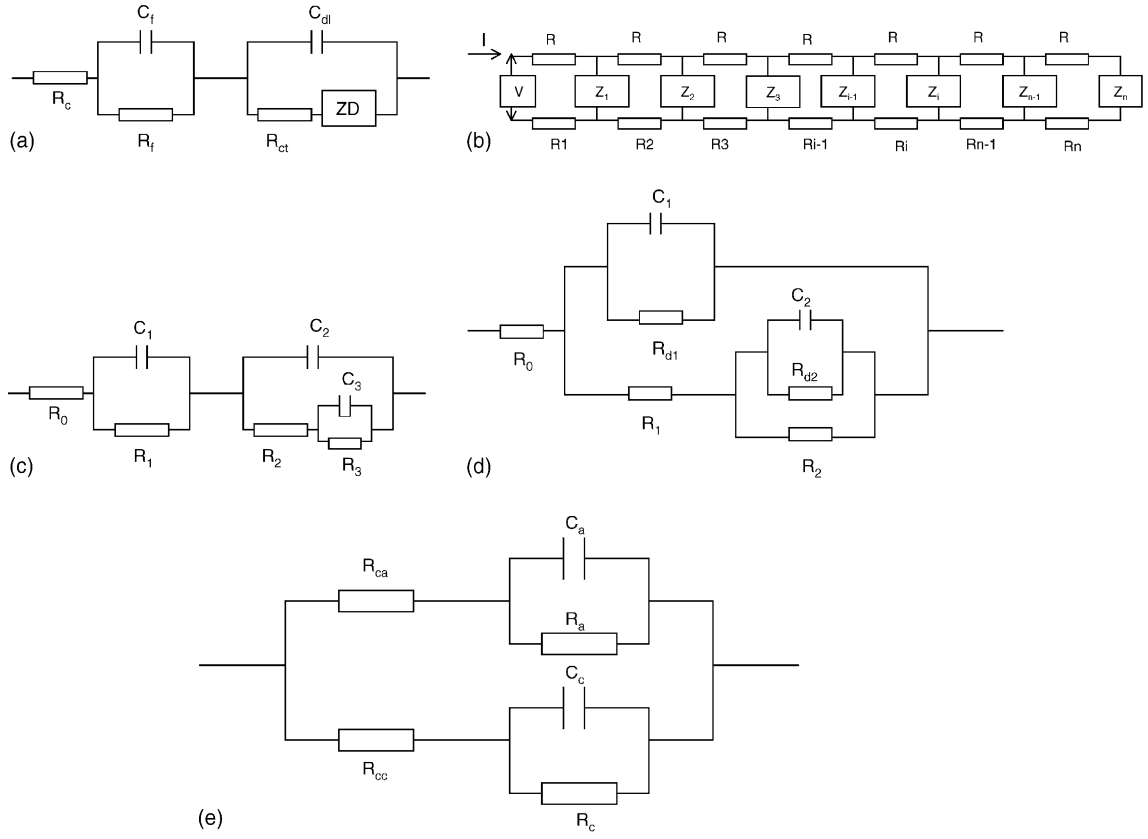

Fig. 6. (a) Equivalent circuit for simulation of impedance data. R_c: concrete resistance; R_f, C_f: film resistance and capacitance; Z_d: diffusional impedance R_{ct}, C_{dl}: charge transfer resistance and double layer capacitance [50]. (b) Discretized transmission line model for rebars in reinforced concrete. R = resistance of rebar/segment; R_j = resistance of concrete/segment; Z_j = rebar/concrete interfacial impedance segment [52]. (c) Equivalent circuit for simulation of impedance data. R_0: concrete resistance; R_1, C_1: resistance and capacitance of a lime-rich layer; R_2, C_2: charge transfer resistance and double layer capacitance; R_3, C_3: resistance and capacitance of an adsorbed intermediate [54]. (d) Equivalent circuit for simulation of impedance data. R_0: concrete resistance; R_1: resistance of products formed on steel; C_1 and R_{d1}: dispersion capacitance and resistance (frequency dependent), accounting for inhomogeneity of concrete surrounding steel; R_2: resistance of steel interface; C_2 and R_{d2}: dispersion capacitance and resistance, accounting for homogeneity of products on metal surface [55]. (e) Equivalent circuit proposed for macrocell corrosion behaviour in reinforced concrete. R_{cc} and R_{ca} = resistance of concrete in cathodic and anodic zones; R_c and R_a = resistance of cathodic and anodic sites; C_c and C_a = capacitance of cathodic and anodic sites [58].

presence of macrocells and presented an alternative circuit [58] as shown in Fig. 6(e), in which two RC networks in parallel allow modelling of rebar macrocell activity.

In spite of the increasing developments in the interpretation of the EIS spectra, sometimes they reveal the presence of features that are difficult to explain. These include: presence of low frequency tails, depressed semicircles and high frequency effects. The first effect led to the introduction of a Warburg element in series with the charge transfer resistance to account for the response of Faradaic processes occurring in the interface. These effects explain why sometimes the steady state cannot be reached with conventional DC techniques, even after long waiting times. They also explain the long time constants observed in the impedance spectra at low frequencies and the need to extrapolate the values of the polarisation resistance.

The high frequency effects are also common in the spectra and have been attributed to several processes, such as the presence of a surface film [50,59]. Montemor et al. [60,61] showed that this time constant is dependent on the presence of additives and could be related with concrete humidity. Another explanation attributes this time constant to polarisation phenomena occurring in saturated concrete [62,63]. The high frequency response also allows determination of concrete resistivity. Fitting of EIS spectra by using an equivalent circuit identical to the one depicted in Fig. 6(a) allowed estimation of the concrete resistivity [60,61]. It was concluded that concrete resistivity in 3% NaCl fully immersed samples was dependent on the time of immersion and on the concrete composition.

The presence of depressed semi-circles suggests a non-ideal behaviour of the capacitors, leading to the introduction of the constant phase element (CPE) in the

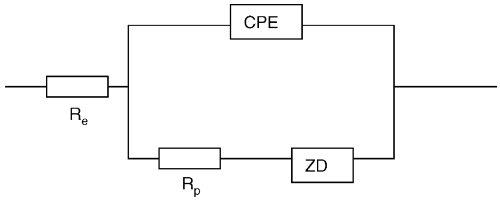

Fig. 7. Equivalent circuit with the introduction of a CPE. R_e = electrolyte resistance; R_p = charge transfer resistance; CPE = constant phase element; ZD = Warburg diffusion [65].

equivalent circuits. Saguës et al. [64] introduced this element in systems exhibiting simple polarisation processes. They concluded that some improvement is obtained if CPE is used instead of an ideal capacitor. In another work, Feliu et al. [65] studied a more complicated process and introduced a CPE and diffusional parameters in the equivalent circuit as shown in Fig. 7. This led to increased accuracy in the determination of the polarisation resistance when that was possible.

The aforementioned features in the EIS spectra were also studied by Ford et al. [66]. By manipulating some parameters of the system, such as specimen geometry, local chemistry and microstructure and electrode schemes, the study assigned three time constants with a number of possible causes. They are: passive films formed on iron, interfacial reactions (polarisation resistance and double layer capacitance) and bulk concrete properties. In some cases, an extra time constant was observed, being attributed to imperfect electrodes due to drying/shrinkage.

The use of EIS as a monitoring technique is still a field under development. It provides substantial information on the characteristics of the system, however sometimes it is difficult to interpret and is a time-consuming technique. Nevertheless, its use is nowadays a powerful tool to understand the behaviour of the steel/concrete system.

3.4. Transient techniques

Application of transient techniques, such as galvanostatic pulse and coulostatic methods, working in the time domain to the steel/concrete system became a common practice in recent years. These techniques are favoured by the relatively slow response of the steel–concrete interface, which makes data collection in the time domain preferable to that in the frequency domain (as in EIS). Another advantage of the techniques is that they can provide the values of the polarisation resistance and double layer capacitance from the measurement of a time constant per unit area, being independent of the total steel area under measurement. This becomes an advantage for in situ monitoring over other techniques that need the knowledge of the system area.

In galvanostatic pulse technique (GPT) a small current perturbation (I_{ap}) is applied to the reinforcing steel using an auxiliary electrode on the concrete surface in a similar manner as in linear polarisation measurements. The response, a potential transient (V_t), is then recorded as shown in Eq. (4).

$$V_t = I_{ap}.R_\Omega + I_{ap}.R_p[1 - \exp(-t/(R_p.C_{dl}))] \quad (4)$$

where t is the time, R_p and C_{dl} are the polarisation resistance and the double layer capacitance at the steel bar surface, respectively, and R_Ω is the ohmic resistance between surface electrode and the steel bar.

The detailed analysis and fitting of the system response allows determination of parameters of the equivalent circuit and calculation of the corrosion rates.

In a review about electrochemical techniques applied to corrosion monitoring of steel in concrete, Gonzalez et al. [51] pointed some difficulties in adopting non-steady-state transient methods: they may result in overestimation or underestimation of the corrosion rate. Following this line of research, Feliu et al. [67] made some preliminary studies on the transient response (TR) analysis applied to reinforcing steel. The work shows that the technique can be an alternative to EIS for determining the ohmic resistance, double layer capacitance and polarisation resistance. In 1988, Newton and Sykes [68] published a study where GPT, was employed to examine the impedance response of reinforcing steel immersed in seawater. The work shows that using GPT the contributions from diffusion and polarisation resistance that are usually superimposed in the impedance spectra can be more easily individualised.

Gowers and Millard [69] applied pulse-mapping techniques for corrosion monitoring of reinforced concrete structures and found that the response to a galvanostatic pulse was mainly determined by the concrete resistance, through which the pulse is passing. As such, the technique essentially produces a map of concrete resistivity. The authors recommend that the technique should be used together with potential mapping because wrong interpretation can arise if the pulse mapping is performed on sites where potential mapping indicate little chance of corrosion.

Elsener et al. [70,71] applied GPT on-site, on concrete walls heavily contaminated with chlorides from de-icing salts up to 1 m height. Fig. 8 shows the potential time transients measured in that wall. The curves obtained at the bottom (corroding area) show a small ohmic drop and quickly reach the steady-state potential. The results obtained with this technique are summarised in Table 1. The technique proved to be effective allowing determination within a few seconds of the open circuit potential, ohmic resistance and polarisation resistance. It also allows combined potential and resistivity mapping since the ohmic resistance is proportional to concrete resis-

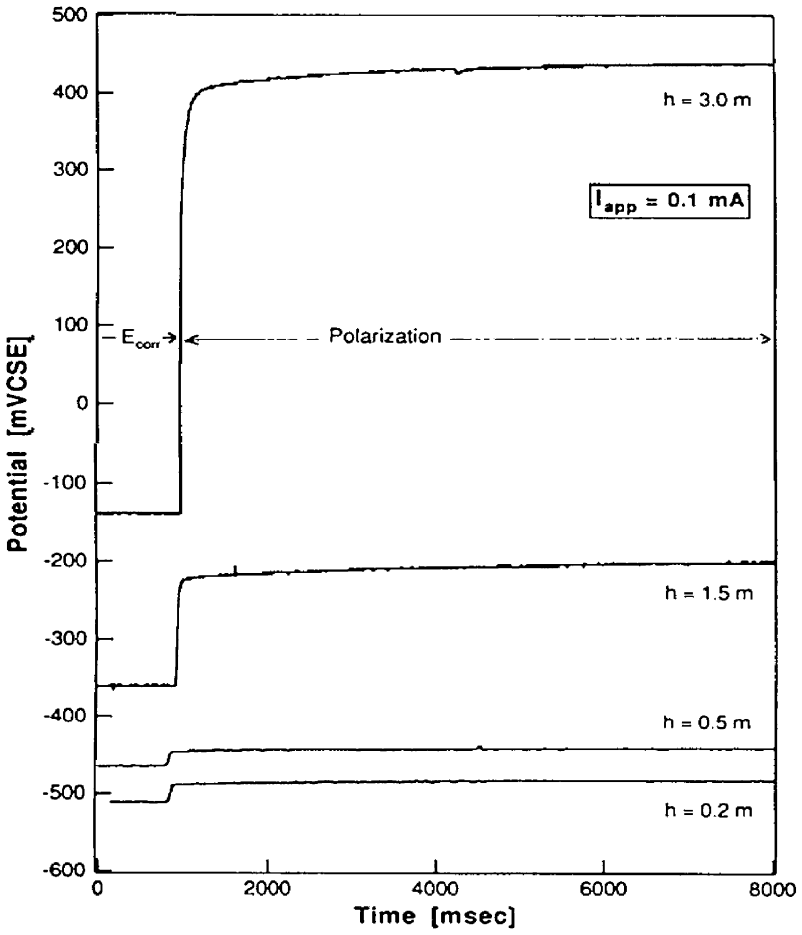

Fig. 8. Galvanostatic pulse transients measured at different heights on a reinforced concrete wall heavily contaminated up to 1 m, current $I_{app} = 0.1$ mA [70]. Results see Table 1.

Table 1
Results of the Galvanostatic pulse measurements on a reinforced concrete wall exposed to splash water with deicing salts

Height (m)	E_{corr} (mV (SCE))	$I_{ap}.R_p + I_{ap}.R_\Omega$ (mV (SCE))	R_Ω (Ω)	R_{peff} (Ω)	T_{const} (s)	R_p (k Ω cm^2)
0.2	−510	−483	220	60	2.25	10
0.5	−482	−462	160	38	2.47	7
1.5	−360	−200	1380	235	3.36	800
3.0	−138	+442	5350	430	4.25	2000

Heavily chloride contaminated up to 1 m height [70].

tivity and facilitated identification of the points where high corrosion risk exists.

The corrosion rate is proportional to the inverse of the time constant (if the capacitance per unit area remains constant) and its variation allows the knowledge of the corrosion state. Glass et al. [72] examined the sensivity of the time constants to corrosion rate and observed that the shape of the transients was modified with changes in the corrosion rate. However, the decay was not an exponential function, as expected if the process was determined by charge transfer reactions. Faced with these changes, the authors proposed an empirical equation that fitted the transients more accurately. Later, Glass [73] studied potential-time transients on active and passive steel following the application of a short current pulse. The various corrosion rates were induced by periodically exposing the samples to 5% NaCl. The measurements detected two transient processes; the slower one being strongly dependent on the steel condition, as shown in Fig. 9. The transient obtained on the passive specimens exhibit a much slower decay than that obtained on the active ones. The curves of Fig. 9 were fitted to 90% by using the exponential law and the calculated R_p values were 2.76 and 338 Ω m^2 for

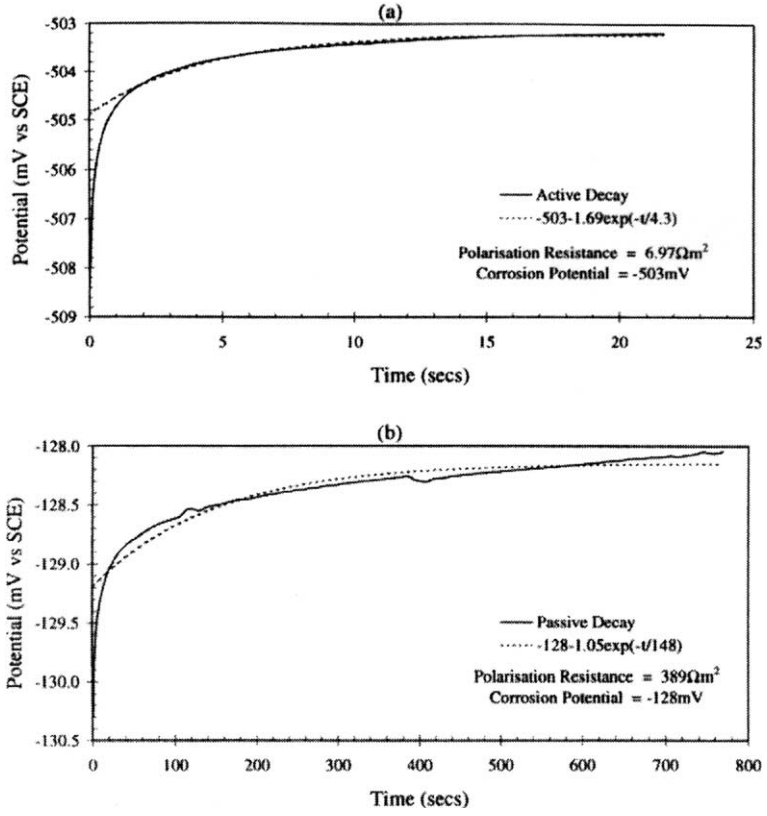

Fig. 9. Slow coulostatic transient obtained on (a) active and (b) passive steel in concrete. The potential decay shown represents 90% of the potential shift at 1 s (Note the different × scales). From Ref. [73].

the active and passive steel, respectively. The values obtained using DC polarisation were 6.97 and 389 $\Omega\,m^2$, respectively. The authors used an alternative approach to the fitting, which consists in the measurement of the time constant directly from the capacitance, a method that is less time consuming. With this procedure the values of R_p were 4.14 and 435 $\Omega\,m^2$ for the active and passive steel, respectively. This procedure has the advantage to use the time constant that is corrosion rate sensitive and is expected to be independent of the area.

Some advantages of the transient methods also include [73,74]: a small perturbation during which the effects of diffusion can be minimised by keeping the perturbation period short; no need to compensate the result for the effects of the electrolyte resistance; determination of the interface capacitance; its suitability for low frequency work when compared to EIS. Disadvantages, however, include long time to obtain the transient when compared to DC polarisation, particularly for passive steel.

In a recent work [75] GPT was applied to samples under exposure at an urban maritime city (Liverpool), including specimens with stainless steel to simulate passive systems and results were compared with DC polarisation. The work shows that corrosion rates calculated from DC polarisation are somewhat lower than those obtained with GPT. Differences fell within a factor of 2.5 for the active states. The study shows that GPT enables different electrical capacitive and resistive components of the system to be resolved. The technique distinguishes between active and passive steel and allows identification of resistive components resulting from the dielectric properties of the system and its discount on corrosion rates calculations. The data obtained suggest that the presence of components from bulk effects within concrete may induce errors in conventional DC measurements.

4. Conclusions

The composition of the passive film formed on reinforcing steel and the mechanism of its breakdown by chlorides can be explained by more than one model. However it can be assumed that chloride ion form soluble complexes with iron leading to localised acidification and consequent pit growth.

Chlorides can bind with concrete, being partially immobilised in the matrix. In spite of this, bound chloride may participate in the corrosion process if the pH falls, leading to dissolution of the chloride complexing phases.

Potential mapping is a helpful technique to detect corroding rebars and is recommended as a first approach to study the system. The technique proved to be applicable to on-site monitoring, but results need to be interpreted with care, especially under restricted oxygen supply.

DC polarisation measurements are able to calculate the polarisation resistance. Accuracy of the technique is significantly improved by the use of measuring devices working on the principle of the guard ring technique. The development of portable and easy-operation monitoring systems makes the technique adequate for rapid on-site determination of the corrosion rate.

EIS is a powerful technique to study the steel/concrete system. It provides information on a number of parameters, such as the presence of surface films, bulk concrete characteristics, interfacial corrosion and mass-transfer phenomena. However, interpretation of the results can be a difficult task and the need of an equivalent circuit that can change with steel condition, makes the technique more suitable for laboratory studies. The technique is also time consuming. Nevertheless, its use is of fundamental interest for detailed knowledge of the steel/concrete system.

Transient methods working in the time domain have proved to be effective for on-site monitoring. These techniques are rapid and non-destructive and provide information on steel condition as well as information on concrete resistivity. The presence of processes other than activation-controlled processes may cause deviations from the expected exponential behaviour and consequently makes it difficult to estimate system-related parameters, which may result in underestimation or overestimation of the corrosion rate.

Acknowledgements

The authors acknowledge the support from POCTI.

References

[1] Tuutti K. In: Corrosion of steel in concrete. Stockholm, Sweden: Swedish Cement and Concrete Research Institute; 1982.
[2] Pourbaix M. Atlas of electrochemical equilibria in aqueous solutions. Oxford: Pergamon Press; 1966.
[3] Hansson CM. Cem Concr Res 1984;14:574.
[4] Nagayama M, Cohen M. J Electrochem Soc 1963;110:670.
[5] Kruger J, Calvert JP. J Electrochem Soc 1967;114:43.
[6] Metha. In: Malhotra VM, editor. Proceedings of the Second International Conference On Durability of Concrete, Montreal, Canada, vol. 1, SP126-1. 1991. p. 1.
[7] Oranowska H, Szklarska-Smialowska Z. Corros Sci 1981;21:735.
[8] Zakroczymski T, Fan C-J, Szklarska-Smialowska Z. J Electrochem Soc 1985;132:2862.
[9] Zakroczymski T, Fan C-J, Szklarska-Smialowska Z. J Electrochem Soc 1985;132:2868.
[10] Belaid F, Arliguie G, François R. Corrosion 2000;56(9):960.
[11] Page CL. Nature 1975;258:514.
[12] Khalaf MN, Page CL. Cem Concr Res 1979;9:197.
[13] Page CL, Treadway KWJ. Nature 1982;297:109.
[14] Leek DS, Poole AB. In: Page CL, Treadway KW, Bamforth PB, editors. Proceedings of the Third International Symposium On Corrosion of Reinforcement in Concrete. London: Elsevier Applied Science; 1990. p. 67.
[15] Montemor MF, Simões AMP, Ferreira MGS. Corrosion 1998;54(5):347.
[16] Jovancicevic V, Bockris JOM, Carbajal JL, Zelenay P, Mizuno T. J Electrochem Soc 1986;133:2219.
[17] Leckie HP, Uhlig HH. J Electrochem Soc 1966;113:1262.
[18] Leckie HP, Uhlig HH. J Electrochem Soc 1969;116:906.
[19] Kolotorkyn YM. J Electrochem Soc 1961;108:209.
[20] Hoar TP. Corros Sci 1967;7:355.
[21] Sato N. J Electrochem Soc 1982;129:255.
[22] Chao CY, Lin LF, MacDonald DD. J Electrochem Soc 1981;128:1194.
[23] Pou TE, Murphy OJ, Young V, Bockris JOM, Tongson LL. J Electrochem Soc 1984;131:1243.
[24] Grady WEO, Bockris JOM. Surf Sci 1973;10:245.
[25] Suryavanshi AK, Scantelbury JD, Lyon SB. Cem Concr Res 1996;26:717.
[26] Sanjuán MA. Corros Sci 1999;41:335.
[27] Schiessl P, Raupach M. In: Page CL, Treadway KW, Bamforth PB, editors. Proceedings of the Third International Symposium On Corrosion of Reinforcement in Concrete. London: Elsevier Applied Science; 1990. p. 49.
[28] Glass GK, Buenfeld NR. In: Nilsson LO, Olivier JP, editors. Chloride penetration in concrete. Paris: Pub. RILEM; 1997. p. 429.
[29] Glass GK, Buenfeld RN. Corros Sci 1997;39:1001.
[30] Glass GK, Buenfeld NR. Corros Sci 2000;42:329.
[31] Glass GK, Reddy B, Buenfeld NR. Corros Sci 2000;42:1587.
[32] Arup H. In: Crane AP, editor. Corrosion of reinforcement in concrete construction. UK: London; 1983. p. 151.
[33] Elsener B, Böhni H. Mater Sci Forum 1992;111/112:635.
[34] Montemor MF, Simões AMP, Salta MM. Cem Concr Compos 2000;22:175.
[35] Browne RD, Geoghegan MP, Baker AF. In: Crane AP, editor. Corrosion of reinforcement in concrete construction. UK: London; 1983. p. 193.
[36] Alonso C, Andrade C, Izquierdo M, Nóvoa XR, Perez MC. Corros Sci 1998;40:1379.
[37] Broomfield JP. In: Swamy RN, editor. Corrosion and corrosion of steel in concrete, vol. 1. UK: Sheffield; 1994. p. 1.
[38] Grimaldi G, Brevet P, Pannier G, Raharinaivo A. Brit Corros J 1986;21:55.
[39] Stern M, Geary AL. J Electrochem Soc 1957;104:56, pp. 390, 561, 645.
[40] Feliu S, Gonzalez JA, Andrade C, Feliu V. Corrosion 1998; 44:761.
[41] Feliu S, Gonzalez JA, Andrade C, Feliu V. Corros Sci 1989; 29:105.
[42] Gonzalez JA, Feliu S, Andrade C, Rodriguez I. Mater Struct/ Materiaux et Constr 1991;24:346.
[43] Ahmad S, Bhattacharjee B. Corrosion 1995;37:1995.
[44] Feliu S, Gonzalez JA, Escudero ML, Feliu Jr S, Andrade C. Corrosion 1990;46:1015.
[45] Sehgal A, Li D, Kho YT, Osseo-Asare K, Pickering HW. Corrosion 1992;48:706.
[46] Feliu S, Gonzalez JA, Feliu Jr S, Andrade C. ACI Mater J 1990;(Sept/Oct):457.
[47] Hladky K, John DG, Dawson JL. Developments in Rate of Corrosion Rate Measurements for Reinforced Concrete Structures, UK Corrosion 90, UK, 1990.

[48] Flis S, Sobol S, Pickering HW, Sehgal A, Osseo-Asare K, Cady PD. Corrosion 1993;49:601.
[49] Videm K, Myrdal R. Corrosion 1997;53:734.
[50] John DG, Searson PC, Dawson JL. Brit Corros J 1981;16:102.
[51] Gonzalez JA, Molina A, Escudero ML, Andrade C. Corros Sci 1985;25:519.
[52] Macdonald DD, McKubre MCH, Urquidi-Macdonald M. Corrosion 1988;44:2.
[53] Saguës AA. NACE Corrosion 190, 1990, 132, Las Vegas, Nevada, USA.
[54] Wenger F, Galland J. Mater Sci Forum 1989;44&45:375.
[55] Dhouibi L, Trikki E, Grandet J, Raharinaivo A. Cem Concr Res 1996;26:253.
[56] Nöggerath J, Böhni H. Mater Sci Forum 1989;44&45:357.
[57] Keddam M, Nóvoa XR, Soler L, Andrade C, Takenouti H. Corros Sci 1994;36:1155.
[58] Nóvoa XR, Izquierdo M, Espada L. Rev Iberoam Corros Prot 1987;26:237.
[59] Lay P, Lawrence PF, Wilkins NJM. J Appl Electrochem 1985;17:755.
[60] Montemor MF, Simões AMP, Salta MM, Ferreira MGS. Corros Sci 1993;35:1571.
[61] Montemor MF, Simões AMP, Salta MM, Ferreira MGS. In: Swamy RN, editor. Corrosion and corrosion protection of steel in concrete. UK: Sheffield; 1994. p. 571.
[62] Carter WJ, Garvin SJ. J Phys D 1984;22:1173.
[63] Keddam M, Takenouti H, Nóvoa XR, Andrade C, Alonso C. Mater Sci Forum 1998;289–292:15.
[64] Saguës AA, Kranc SC, Moreno EI. Corros Sci 1995;37:1097.
[65] Feliu V, Gonzalez JA, Andrade C, Feliu S. Corros Sci 1998;40:975.
[66] Ford SJ, Shane JD, Mason TO. Cem Concr Res 1998;28:1737.
[67] Feliu S, Gonzalez JA, Andrade C, Feliu V. Corros Sci 1986;26:961.
[68] Newton CJ, Sykes JM. Corros Sci 1988;28:1051.
[69] Gowers KR, Millard SG. In: Swamy RN, editor. Corrosion and corrosion protection of steel in concrete. UK: Sheffield; 1994. p. 186.
[70] Elsener B, Wojtas H, Böhni H. In: Swamy RN, editor. Corrosion and corrosion protection of steel in concrete. UK: Sheffield; 1994. p. 236.
[71] Elsener B, Wojtas H, Böhni H. In: Proc Corrosion 95, Houston, Texas. 1995. p. 3260.
[72] Glass GK, Page CL, Short NR, Yu SW. Corros Sci 1993;35:1585.
[73] Glass GK. Corros Sci 1995;37:597.
[74] Glass GK, Page CL, Short NR, Zhang JZ. Corros Sci 1997;39:1657.
[75] Law DW, Millard SG, Bungey JH. Corrosion 2000;56:48.